g factors of ^{17}N and ^{18}N remeasured

M. De Rydt,[1] D. L. Balabanski,[2] J. M. Daugas,[3] P. Himpe,[1] D. Kameda,[4] R. Lozeva,[1,*] P. Morel,[3] L. Perrot,[5] K. Shimada,[6] C. Stödel,[7] T. Sugimoto,[4] J. C. Thomas,[7] H. Ueno,[4] N. Vermeulen,[1] P. Vingerhoets,[1] A. Yoshimi,[4] and G. Neyens[1]

[1]*Instituut voor Kern- en Stralingsfysica, K. U. Leuven, Celestijnenlaan 200D, B-3001 Leuven, Belgium*

[2]*Institute for Nuclear Research and Nuclear Energy, Bulgarian Academy of Sciences, BG-1784 Sofia, Bulgaria*

[3]*CEA, DAM, DIF, F-91297 Arpajon Cedex, France*

[4]*RIKEN Nishina Center, 2-1 Hirosawa, Wako, Saitama 351-0198, Japan*

[5]*IPN, 15 Rue G. Clemenceau, F-91406 Orsay, France*

[6]*CYRIC, Tohoku University, 6-3 Aoba, Aramaki, Aoba-ku, Sendai, Miyagi 6980-8578, Japan*

[7]*Grand Accélérateur National d'Ions Lourds (GANIL), CEA/DSM-CNRS/IN2P3, B. P. 55027, F-14076 Caen Cedex 5, France*

(Received 14 July 2009; published 22 September 2009)

The g factors of the ^{17}N and ^{18}N ground states were remeasured using the β-nuclear magnetic resonance (β-NMR) technique on spin-polarized fragment beams at the LISE fragment separator at GANIL. Based on the g-factor results, the magnetic moments of ^{17}N ($I^\pi = 1/2^-$) and ^{18}N ($I^\pi = 1^-$) were deduced: $|\mu(^{17}\mathrm{N})| = 0.3551(4)\ \mu_N$ and $|\mu(^{18}\mathrm{N})| = 0.3273(4)\ \mu_N$. Both results are in good agreement with and more precise than the earlier observed values.

DOI: 10.1103/PhysRevC.80.037306 PACS number(s): 21.10.Ky, 21.60.Cs, 24.70.+s, 27.20.+n

Exotic nuclei close to the drip lines often exhibit different nuclear properties compared to the isotopes in the valley of stability. Therefore they are extensively studied in theoretical and experimental research, trying to understand the variation in nuclear structure that occurs all over the nuclear chart. A changing shell structure has also been found in the light neutron-rich boron ($Z = 5$), carbon ($Z = 6$), nitrogen ($Z = 7$), and oxygen ($Z = 8$) isotopes (e.g., [1–6]). For these nuclei, monopole interactions vary rapidly as the $\pi(p)$ shell and the $\nu(sd)$ orbitals are filled, giving rise to new shell gaps and vanishing magic numbers.

An earlier β-NMR measurement on $^{17}_{7}\mathrm{N}_{10}$ ($I^\pi = 1/2^-$, $t_{1/2} = 4.173$ s [7]) showed that configurations with two sd neutrons coupled to $J^\pi = 2^+$ are present in the ground state. This induces a larger magnetic moment than the Schmidt value [8] for an odd $p_{1/2}$ proton [9]. For $^{18}_{7}\mathrm{N}_{11}$ ($I^\pi = 1^-$ [10], $t_{1/2} = 619(2)$ ms [11]), the ground state properties and the β decay are extensively discussed in Refs. [10–19]. Large-scale shell-model calculations suggest a ground-state structure dominated by configurations with three unpaired $d_{5/2}$ neutrons coupled to $J^\pi = 3/2^+$, turning ^{18}N into a transition nucleus toward the deformed $^{17}_{6}\mathrm{C}_{11}$ isotope [20]. Note that two contradictory magnetic and quadrupole moments have been reported: $|\mu|_1 = 0.3279(13)\ \mu_N$, $|Q|_1 = 12.3(12)$ mb in Ref. [14] and $|\mu|_2 = 0.135(15)\ \mu_N$, $|Q|_2 = 27(4)$ mb in Ref. [15]. This often suggests the presence of an isomeric state in the isotope of interest. A sufficiently long lifetime of the isomer (typically $\geqslant 50\ \mu$s) is required in order to induce a visible β-NMR resonance effect. The lower lifetime limit is determined by the applied radio-frequent-field strength.

Although a 5.25 μs isomer is observed in ^{16}N [7] and shape coexistence is predicted to occur in ^{17}C [5], no experimental evidence has been found for the presence of a long-lived ($\geqslant 50\ \mu$s) isomeric state in ^{18}N. So far, the level scheme of ^{18}N has been studied in three types of experiments, probing the charge-exchange reaction ^{18}O(^{7}Li, ^{7}Be)^{18}N [12], the β decay of ^{18}C [21] and the fusion-evaporation reaction ^{9}Be(^{11}B,2p)^{18}N [19]. In the charge-exchange reaction, excited states were observed with a resolution of 10 keV only, revealing two strongly populated levels around 121 keV and 747 keV, a weakly populated level at 580 keV, and two levels above 2 MeV (left panel of Fig. 1). The spin assignments, shown in Fig. 1, were made by Barker based on a weak-coupling model [22]. In the β decay of ^{18}C, states at 115 keV and 587 keV could be identified (middle panel of Fig. 1), close in energy to the lowest states observed in the charge-exchange reaction. The decay intensity of the 115 keV level to the ground state was found to be more than a factor two lower than expected from the analysis of the full data set. It was suggested that this is due to a nonobserved long-lived isomeric transition in ^{18}N. In the fusion-evaporation reaction, three levels were observed at 115 keV, 587 keV, and 742 keV, respectively (right panel of Fig. 1). The lifetimes of these states were measured using the recoil distance method [23]. The 115 keV level has a lifetime of 582(165) ps while the other two have lifetimes below 40 ps. The technique used in this experiment was not sensitive to long-lived isomers because of the short time window (100 ns) used for correlations between the γ-rays and the two protons. Since the presence of an isomeric state in ^{18}N has not been confirmed so far, the discrepancy between the two measured sets of nuclear moments remains unclarified.

In this Brief Report we report on a new measurement of the magnetic moments of ^{17}N and ^{18}N performed during a test experiment which was meant to evaluate the performance of a new β-NMR setup installed at the LISE beam line [24,25] at GANIL. A technical description of the setup will be published elsewhere [26].

*Present address: CSNSM, Université Paris-Sud 11, CNRS/IN2P3, F-91405 Orsay Campus, France.

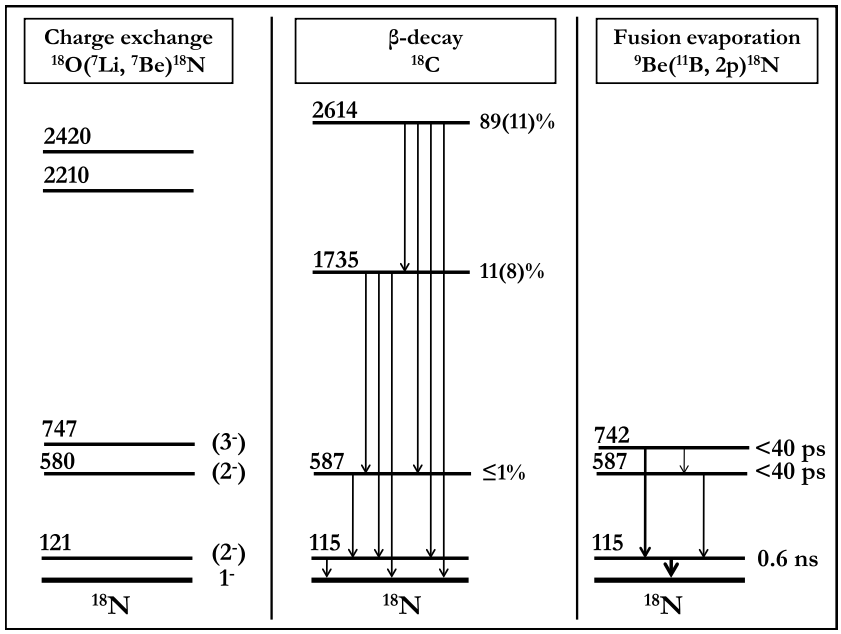

FIG. 1. Level schemes of ^{18}N proposed in (left) the charge-exchange reaction ^{18}O(^{7}Li, ^{7}Be)^{18}N [12], (middle) the β decay of ^{18}C [21], (right) the fusion-evaporation reaction ^{9}Be(^{11}B,2p)^{18}N [19].

Both N fragments were produced in an intermediate energy reaction, induced by a $^{18}O^{8+}$ primary beam (1 μA, 74.3A MeV) on a 1182μm ^{9}Be target. Spin-polarization of the $^{17-18}$N-fragments was obtained by putting an angle of 2(1)$^\circ$ on the primary beam with respect to the entrance of the spectrometer and by making a selection in the longitudinal momentum distribution. The ^{17}N isotopes were produced by a projectile-fragmentation reaction for which the highest spin-polarization is known to occur in the wings of the momentum distribution [27–29]. For single nucleon pick-up reactions, such as the production mechanism of the ^{18}N fragments, it was demonstrated that a large amount of polarization is achieved in the left wing and in the center of the momentum distribution [30]. Selecting a momentum window according to these conditions resulted in about 2×10^5 polarized ^{17}N-ions per second and about 10^5 polarized ^{18}N-ions per second at the final focal point of the LISE fragment separator. A purity of 94% was achieved for both secondary beams, using a 1020 μm ^{9}Be wedge degrader in the intermediate dispersive plane. During the beam-tuning process, the transmission of the secondary beam was monitored on three Si detectors, using the standard energy loss versus time-of-flight technique.

In the β-NMR setup, the selected secondary beam is stopped in a 2 mm MgO crystal at room temperature. The β particles, produced by the decay of the implanted fragments, are detected in two $\Delta E/E$ pairs of plastic scintillators. Both pairs are situated along the vertical polarization direction, one above the crystal, the other below. When a polarized ensemble of nuclei decays, an anisotropic β-radiation pattern is emitted and the observed β asymmetry A is given as

$$A = \frac{N(0^\circ) - N(180^\circ)}{N(0^\circ) + N(180^\circ)} \simeq \frac{v_\beta}{c} A_\beta P. \qquad (1)$$

P is the polarization of the selected ensemble and A_β is the asymmetry parameter determined by the β-decay properties (e.g., the initial and final spins) of the nuclei under investigation. The ratio of the velocity of the β particles, v_β, to the speed of light can be taken as 1 since ^{17}N and ^{18}N have high Q_β values [$Q_\beta(^{17}\mathrm{N}) = 8.68$ MeV and $Q_\beta(^{18}\mathrm{N}) = 13.9$ MeV]. When the spin polarization of the implanted ensemble is destroyed, a change in the β-asymmetry detection, proportional to $A_\beta P$, is observed.

In the case of β-NMR, the spin polarization is resonantly destroyed by hyperfine interactions between the nuclear spin ensemble and the static and radiofrequent (rf) magnetic fields. The static magnetic field B_0, applied along the polarization direction, induces an equidistant (Zeeman) splitting of the nuclear m states. The energy difference between two subsequent levels is proportional to the nuclear g factor and the magnetic field strength: $\Delta E = g\mu_N B_0$. Perpendicular to B_0, a rf field with frequency ν is generated inside a coil placed around the crystal. When the energy $h\nu$ of the rf field equals the energy difference between two quantum levels, equal populations of all m states are induced, resulting in an isotropic ensemble and a zero β asymmetry. This happens when the rf frequency corresponds to the Larmor frequency ν_L:

$$\nu_L = \frac{g\mu_N B_0}{h}. \qquad (2)$$

By scanning the β asymmetry as a function of the rf frequency, the nuclear g factor can be deduced from the position of the observed resonance.

While the polarized beam is implanted continuously, the rf frequency is changed in discrete steps every 10 sec to 1 min, depending on the lifetime. In order not to miss out on the resonance frequency, each applied rf frequency is modulated around its central value. The modulation range covers at least one-half of the interval between two subsequent central frequencies and is repeated at a rate of 100 Hz. After applying all frequencies in a certain scan range, data without rf field are taken as a reference. The complete cycle is repeated until enough statistics are obtained. Depending on the production rate and the detection efficiency, this takes 30 min up to a few hours.

During the β-NMR measurement, the static magnetic field B_0 is monitored by the hall probe which is positioned at about 7 cm behind the implantation crystal. From the recorded field value, the field strength at the position of the crystal can be calculated, relying on the magnet calibrations performed before and after the experiment. Using the average of both calibration curves, a field value of 0.15967(12) T was obtained for the ^{17}N measurements while B_0 was 0.39971(33) T for the β-NMR's on ^{18}N. The errors on these values consist of two contributions, added in quadrature. The statistical contribution includes the error on the field measured at the hall probe position and the errors on the slope and the intercept of the calibration function. The systematic error is given by the 0.1 mT and 0.25 mT divergence observed for repeated calibrations around 0.16 T and 0.4 T, respectively.

Three β-NMR measurements were performed on the ground state of ^{17}N. Initially, a broad frequency region was scanned in steps of 10 kHz with 6 kHz modulation (Fig. 2(a)), revealing a 0.56(6)% NMR effect at $\nu_{L,1} = 864.7(20)$ kHz. Two fine scans around the observed resonance confirmed this result. The first fine scan was performed by scanning a narrow rf-frequency range in steps of 4 kHz with a modulation of 2.5 kHz (Fig. 2(b)). A Larmor frequency of $\nu_{L,2} = 864.7(7)$ kHz was obtained. The same rf region was studied by a second fine scan, applying frequencies which were only 2 kHz apart and a modulation of 3 kHz. This resulted in a Larmor frequency $\nu_{L,3} = 863.1(15)$ kHz (Fig. 2(c)). The function used to fit the three β-NMR curves includes the Lorentzian line shape and the modulation [31] with the resonance frequency, the position of the baseline, the FWHM of the Lorentz curve and the amplitude of the resonance as fit

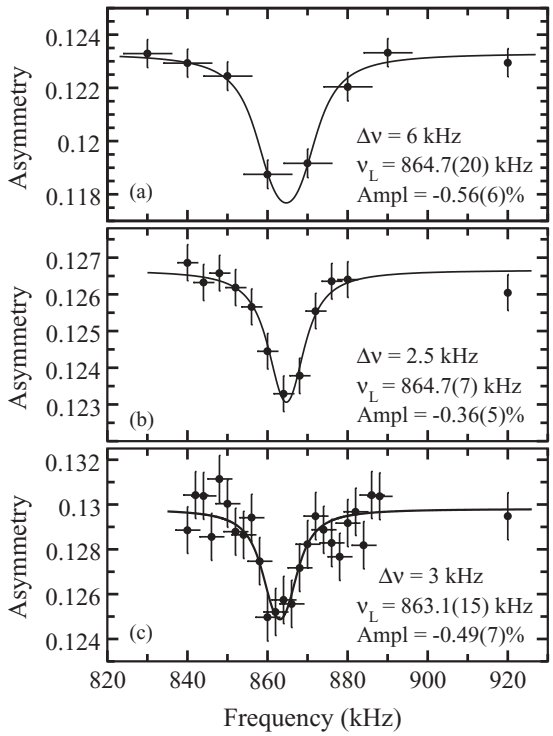

FIG. 2. β-NMR results for ^{17}N. (a) Broad scan with step 10 kHz. (b) Fine scan with step 4 kHz. (c) Fine scan with step 2 kHz.

TABLE I. Resonance frequencies and amplitudes for the β-NMR's on ^{18}N. The measurements were performed for different momentum selections.

Momentum selection [slit positions]	ν_L (kHz)	Amplitude
Left wing [−45; −25]	997.1(13)	0.57(10)%
Center + right wing [−20; −5]	998.5(21)	0.37(9)%
Right wing [−5; +15]	996.5(30)	0.31(11)%

parameters. The outer right point in each β-NMR spectrum contains the data taken without the rf field.

The weighted mean of the measured Larmor frequencies is calculated to be $\overline{\nu}_L(^{17}\mathrm{N}) = 864.4(6)$ kHz. Consequently, the experimental results for the g factor and the magnetic moment of ^{17}N are $|g(^{17}\mathrm{N})| = 0.7102(7)$ and $|\mu(^{17}\mathrm{N})| = |g|I\mu_N = 0.3551(4)\ \mu_N$, respectively. The diamagnetic correction factor for N isotopes in a MgO crystal equals $+3.55(20) \times 10^{-4}$ ([32] and references therein). Since the induced effect is smaller than the quoted error on the ^{17}N magnetic moment, no diamagnetic correction is performed. The obtained magnetic moment is in agreement with and five times more precise than the published value $|\mu(^{17}\mathrm{N})|_{\mathrm{publ.}} = 0.352(2)\ \mu_N$ [9]. An extensive discussion and interpretation of the ^{17}N result can be found in Ref. [9].

To study the g factor(s) of ^{18}N, the region around the earlier observed value $g = 0.3279(13)$ [14] was scanned three times. In each measurement, seven central frequencies were applied in steps of 16 kHz with a modulation of 10 kHz. Three different settings of the momentum slits were used, resulting in a different initial polarization for each β-NMR measurement. A summary of the β-NMR results is given in Table I and the resonance with the highest amplitude is shown in Fig. 3.

The weighted mean of the three ^{18}N Larmor frequencies is calculated to be $\overline{\nu}_L(^{18}\mathrm{N}) = 997.3(10)$ kHz. Based on this result, the g factor of ^{18}N can be established: $|g(^{18}\mathrm{N})| = 0.3273(4)$. Assuming that this value corresponds to the g factor of the 1^- ground state, $|\mu(^{18}\mathrm{N})| = 0.3273(4)\ \mu_N$ is obtained, in excellent agreement with the value $|\mu(^{18}\mathrm{N})|_{\mathrm{publ.}} = 0.3279(13)\ \mu_N$, published by Ogawa *et al.* in Ref. [14]. The result does not include a diamagnetic correction. Due to the

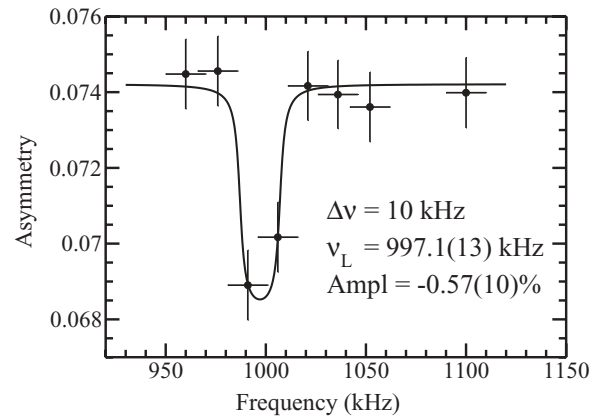

FIG. 3. β-NMR result for ^{18}N.

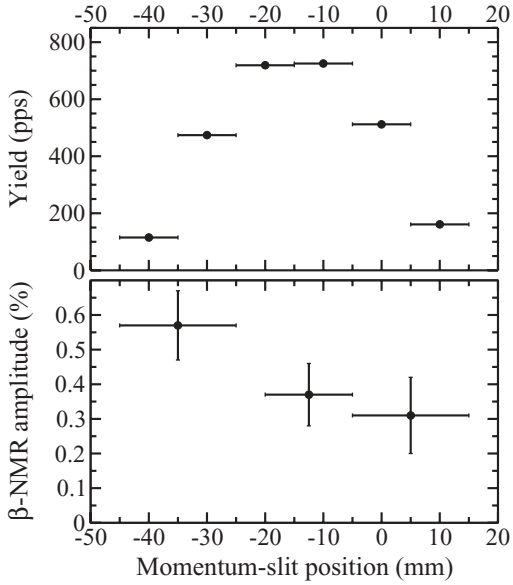

FIG. 4. ^{18}N production yields (upper panel) and β-NMR amplitudes (lower panel) as a function of the momentum-slit position. The position and the opening of the slits are indicated with a horizontal error bar.

limited amount of beam time, the g-factor range corresponding to the result proposed by Neyens *et al.* in Ref. [15] could not be investigated in detail. A new measurement of that g-factor region would clarify the discrepancy between both experimental magnetic moments and it would confirm whether or not a long-lived isomer occurs in ^{18}N. A thorough analysis and discussion of the ^{18}N result can be found in [14] and will not be repeated here.

The upper panel of Fig. 4 gives the ^{18}N pick-up production yield for several momentum selections, applying a primary beam intensity of about 4 nA. In the lower panel, the resonance amplitudes corresponding to the momentum bins selected in the three β-NMR measurements are shown. In both figures, the position and the opening of the momentum slits are indicated with a horizontal error bar. The identical rf conditions, applied in the β-NMR measurements, allow a direct comparison of the resonance amplitudes, each proportional to the amount of destroyed polarization. Therefore, the curve in the lower panel of Fig. 4 describes the polarization of the nuclear ensemble as a function of the fragment momentum. The curve seems to follow the theoretical trend line [30], which is characterized by a high value of the polarization in the left wing and a gradual decrease when going from the center to the right wing. The large error bars on the amplitude however hinder a clear insight in the detailed behavior of the polarization as a function of the momentum selection.

In conclusion, the magnetic moments of ^{17}N and ^{18}N were measured using the β-nuclear magnetic resonance technique at the LISE fragment separator at GANIL. For the ^{17}N ground state, the magnetic moment $|\mu(^{17}\mathrm{N})| = 0.3551(4)\ \mu_N$ was found. This result is 5 times more accurate than the value published by Ueno *et al.* [9], illustrating that the newly designed β-NMR/β-NQR setup is suited for precision measurements of nuclear moments. For ^{18}N, three β-NMR measurements with different initial polarizations resulted in $|\mu(^{18}\mathrm{N})| = 0.3273(4)\ \mu_N$ which confirms the magnetic moment published by Ogawa *et al.* [14]. A future g-factor measurement around $|g|_2 = 0.135(15)$ should examine the result obtained by Neyens *et al.* [15]. Independently, new β-decay and γ-spectroscopy experiments that allow the observation of a long-lived ($\geqslant$50 μs) isomer are needed. Also a high-precision mass measurement can reveal the presence of an isomeric state in ^{18}N, provided that its half-life is more than 1 ms.

[1] H. Okuno *et al.*, Phys. Lett. **B354**, 41 (1995).
[2] H. Ogawa *et al.*, Eur. Phys. J. A **13**, 81 (2002).
[3] V. Maddalena *et al.*, Phys. Rev. C **63**, 024613 (2001).
[4] M. Stanoiu *et al.*, Phys. Rev. C **78**, 034315 (2008).
[5] H. Sagawa, X. R. Zhou, T. Suzuki, and N. Yoshida, Phys. Rev. C **78**, 041304(R) (2008).
[6] T. Suzuki and T. Otsuka, Phys. Rev. C **78**, 061301(R) (2008).
[7] D. R. Tilley, H. R. Weller, and C. M. Cheves, Nucl. Phys. **A564**, 1 (1993).
[8] G. Neyens, Rep. Prog. Phys. **66**, 633 (2003).
[9] H. Ueno *et al.*, Phys. Rev. C **53**, 2142 (1996).
[10] J. W. Olness, E. K. Warburton, D. E. Alburger, C. J. Lister, and D. J. Millener, Nucl. Phys. **A373**, 13 (1982).
[11] Z. H. Li *et al.*, Phys. Rev. C **72**, 064327 (2005).
[12] G. D. Putt, L. K. Fifield, M. A. C. Hotchkis, T. R. Ophel, and D. C. Weisser, Nucl. Phys. **A399**, 190 (1983).
[13] K. W. Scheller *et al.*, Phys. Rev. C **49**, 46 (1994).
[14] H. Ogawa *et al.*, Phys. Lett. **B451**, 11 (1999).
[15] G. Neyens *et al.*, Phys. Rev. Lett. **82**, 497 (1999).
[16] R. H. France, Z. Zhao, and M. Gai, Phys. Rev. C **68**, 057302 (2003).
[17] L. Buchmann *et al.*, Phys. Rev. C **75**, 012804(R) (2007).
[18] J. L. Lou *et al.*, Phys. Rev. C **75**, 057302(R) (2007).
[19] M. Wiedeking *et al.*, Phys. Rev. C **77**, 054305 (2008).
[20] Z. Elekes *et al.*, Phys. Lett. **B614**, 174 (2005).
[21] M. S. Pravikoff *et al.*, Nucl. Phys. **A528**, 225 (1991).
[22] F. C. Barker, Aust. J. Phys. **37**, 17 (1984).
[23] T. Alexander and J. Forster, *Advances in Nuclear Physics* (Plenum Press, New York, 1978).
[24] R. Anne *et al.*, Nucl. Instrum. Methods Phys. Res. A **257**, 215 (1987).
[25] R. Anne *et al.*, Nucl. Instrum. Methods Phys. Res. B **70**, 276 (1992).
[26] M. De Rydt *et al.* (submitted to Nucl. Instrum. Methods A).
[27] K. Asahi *et al.*, Phys. Lett. **B251**, 488 (1990).
[28] H. Okuno *et al.*, Phys. Lett. **B335**, 29 (1994).
[29] D. Borremans *et al.*, Phys. Rev. C **66**, 054601 (2002).
[30] K. Turzó *et al.*, Phys. Rev. C **73**, 044313 (2006).
[31] D. T. Yordanov, From ^{27}Mg to ^{33}Mg: transition to the island of inversion, Instituut voor Kern- en Stralingsfysica, K. U. Leuven, 2007 (unpublished).
[32] K. Matsuta *et al.*, Phys. Rev. Lett. **86**, 3735 (2001).